

Properties of ZnO films grown on (0001) sapphire substrate using H₂O and N₂O as O precursors by atmospheric pressure MOCVD

Jiangnan Dai, Hongbo Su, Li Wang, Yong Pu, Wenqing Fang, Fengyi Jiang*

Nanchang University, Education Ministry Engineering Research Center for Luminescence Materials and Devices, 235 East Nanjing Road, Nanchang, Jiangxi, 330047, PR China

Received 6 December 2005; received in revised form 27 December 2005; accepted 6 January 2006

Available online 14 March 2006

Communicated by M. Kawasaki

Abstract

In this paper, we compare the properties of ZnO thin films (0001) sapphire substrate using diethylzinc (DEZn) as the Zn precursor and deionized water (H₂O) and nitrous oxide (N₂O) as the O precursors, respectively in the main ZnO layer growth by atmospheric pressure metal–organic chemical vapor deposition (AP-MOCVD) technique. Surface morphology studied by atomic force microscopy (AFM) showed that the N₂O-grown ZnO film had a hexagonal columnar structure with about 8 μm grain diameter and the relatively rougher surface compared to that of H₂O-grown ZnO film. The full-widths at half-maximum (FWHMs) of the (0002) and (10 $\bar{1}$ 2) ω -rocking curves of the N₂O-grown ZnO film by double-crystal X-ray diffractometry (DCXRD) measurement were 260 and 350 arcsec, respectively, indicating the smaller mosaicity and lower dislocation density of the film compared to H₂O-grown ZnO film. Compared to H₂O-grown ZnO film, the free exciton A (FX_A) and its three phonon replicas could be clearly observed, the donor-bound exciton A⁰X (*I*₁₀):3.353 eV dominated the 10 K photoluminescence (PL) spectrum of N₂O-grown ZnO film and the hydrogen-related donor-bound exciton D⁰X (*I*₄):3.363 eV was disappeared. The electron mobility (80 cm²/V s) of N₂O-grown ZnO film has been significantly improved by room temperature Hall measurement compared to that of H₂O-grown ZnO film.

© 2006 Elsevier B.V. All rights reserved.

PACS: 81.15.Gh; 75.55.C; 78.55.–m

Keywords: A1. AFM; A1. Photoluminescence; A1. X-ray diffraction; A3. MOCVD; B1. ZnO

1. Introduction

Due to its wide-gap of 3.37 eV at room temperature, its ultraviolet lasing at room temperature (RT) [1] and its large exciton binding energy of 60 meV [2], ZnO has many potential applications in short wavelength light-emitting devices, such as UV and blue LED/LDs. Many growth techniques for single-crystalline ZnO films have been studied, such as molecular beam epitaxy [3], metal–organic chemical vapor deposition (MOCVD) [4], RF magnetron sputtering [5], and pulsed laser deposition [6]. Among these techniques, MOCVD has many advantages for bulk production and has been proven to be suitable for growth

of many electronic and optoelectronic materials. MOCVD growth of ZnO requires appropriate zinc and oxygen precursors. For the group II element, the mostly used zinc precursor is a metal–organic compound like diethyl or dimethyl zinc (DEZn or DMZn). For the group VI precursor, a large variety of oxygen-containing compounds can be used: gases like O₂, CO₂; water (H₂O) and several types of organic compounds like alcohols, aldehydes, ketons and so on. The somewhat smaller (in comparison to organic oxides) family of inorganic oxynitrides (like N₂O, NO, NO₂) has also attracted attention of researchers as oxygen precursors in the epitaxy of ZnO, since they offer some advantage that they allow the elimination of the unintended carbon and hydrogen incorporation into ZnO during epitaxy. Especially, the behavior of hydrogen in ZnO appears to be a key issue for its electrical properties

*Corresponding author.

E-mail address: jiangfy@ncu.edu.cn (F. Jiang).

according to Refs. [7,8]. Oleynik et al. [9] have demonstrated that the structural and optical qualities of ZnO layers grown on the GaN/Si(1 1 1) templates with N₂O as O precursor are superior to those grown with *iso*-propanol (*i*-PrOH) and acetone by low-pressure MOCVD. The works of Ogata et al. [10] also support the idea that N₂O is a candidate as oxygen precursor. To the best of our knowledge, there have been few reports on the comparative studies on properties of ZnO films on (0001) sapphire with H₂O and N₂O as O precursors by atmospheric pressure MOCVD (AP-MOCVD). In this paper, we compare the surface morphology, crystalline, optical and electrical properties of two kinds of ZnO films grown on c-Al₂O₃ (0001) substrate with H₂O and N₂O as O-precursors by AP-MOCVD.

2. Experimental details

A home-built vertical AP-MOCVD with an in situ laser reflectance monitor system ($\lambda = 635 \text{ nm}$) which has been described in Refs. [11,12] in detail was used for the growth of the ZnO films using 6N-purity DEZn as Zn precursor, deionized water (H₂O) and N₂O as O precursors, and 7N-purity nitrogen as the carrier gas. Typical growth conditions were as follows: The reactor-chamber pressure was 760 Torr. A three-step growth process was proposed. In the first step, a 500 Å ZnO low-temperature buffer layer was grown at 160 °C using DEZn and H₂O as Zn and O precursors, respectively. Here the flow rates were 0.813 and 39 mmol/min. Then the buffer layer was re-crystallized at 800 °C for 5 min. In the second step, the high-temperature ZnO buffer layer was deposited under the growth temperature of 680 °C using DEZn and H₂O as Zn and O precursors too. Here the flow rates are 0.11 and 32.5 mmol/min. In the third step, the main ZnO layer was deposited under the growth temperature of 900 °C using DEZn and N₂O as Zn and O precursors. Here the flow rates are 0.06 and 122 mmol/min. For comparative analysis, another two-step epitaxial growth of ZnO film sample was also prepared using DEZn and H₂O as Zn and O precursors, respectively. Here, the two kinds of samples were marked as sample A and sample B for the ZnO films using N₂O and H₂O as O precursors during the growth of

ZnO main layer, respectively. Fig. 1 shows the detail structures and the VI/II ratios in the growth process of the two samples.

The thickness information of the samples was investigated by the laser in-situ monitor. Surface morphology of the samples was studied by atomic force microscopy (AFM) in a contact mode (Chinese Benyuan Nano Instrument 3100 system). Crystal perfection of the samples was examined by double-crystal X-ray diffractometry (DCXRD) (QC200, BEDE Instruments, UK). The Cu K_α line ($\lambda = 1.54056 \text{ \AA}$) was used as the source, and Ge (004) was used as the monochromator. Photoluminescence (PL) of the samples was measured using the 325-nm line of a He-Cd laser (8 mW) as the excitation source. A closed cycle refrigerator was used to control the temperature from 10 to 150 K. The carrier concentration and mobility of the samples were measured using the van der Pauw method at room temperature, and the Ohmic contacts were made by an indium electrode.

3. Results and discussion

Fig. 2 show the in-situ laser reflectance curves of the two ZnO samples. The regular interference periods appearing in

Sample A	Sample B
Main ZnO(N ₂ O+DEZn,VI/II=2033) (900°C; thickness=1.5μm)	Main ZnO (H ₂ O+DEZn,VI/II=298) (680°C; thickness=2.3μm)
Buffer II (H ₂ O+DEZn,VI/II=298) (680°C; thickness=0.8μm)	Buffer I (H ₂ O+DEZn, VI/II=48) (160°C; thickness=500Å)
Buffer I (H ₂ O+DEZn, VI/II=48) (160°C; thickness=500Å)	
c-Al ₂ O ₃ (0001) substrate	c-Al ₂ O ₃ (0001) substrate

Fig. 1. Structure of the two ZnO samples growth.

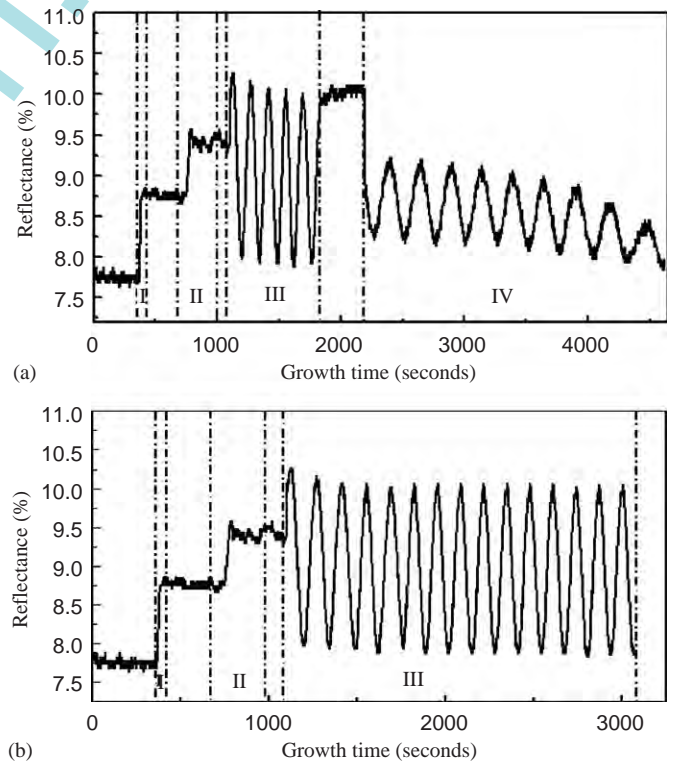


Fig. 2. In-situ laser reflectance curves of the two ZnO samples:(a) Sample A: (I) growth of the low temperature ZnO buffer layer using H₂O as O precursor; (II) re-crystallization at 800 °C for 5 min; (III) growth of the high temperature ZnO buffer layer using H₂O as O precursor; (IV) growth of the main ZnO layer using N₂O as O precursor; (b) Sample B: (I) growth of the low temperature ZnO buffer layer using H₂O as O precursor; (II) re-crystallization at 800 °C for 5 min; (III) growth of the main ZnO layer using H₂O as O precursor.

the traces of two samples indicates that a quasi-two-dimension growth mode has been realized. The thickness for one period can be calculated using the formula

$$2nd = \lambda,$$

where λ is the wavelength of the incident laser, n is the refractive index of ZnO, and d is the thickness of a period. If $n = 2.0$ [13] is used, d can be calculated to be 158.8 nm. For sample A (see Fig. 2(a)), the main successive steps of the growth process are labeled I–IV and delimited by vertical dash lines. Step I is the growth of the low temperature buffer layer at 160 °C, with a reflectivity increase corresponding to a deposited layer thickness of about 500 Å. Step II is re-crystallization of the low buffer

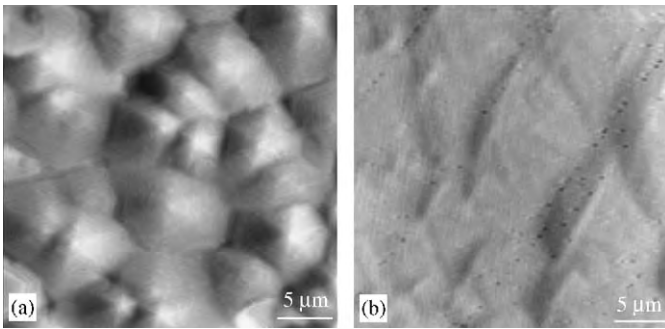


Fig. 3. AFM images of two samples ($25 \mu\text{m} \times 25 \mu\text{m}$): (a) Sample A; (b) Sample B.

layer at 800 °C for 5 min. Step III is the growth of the high temperature ZnO buffer layer. The growth time for each oscillation period is calculated to be 130 s from the reflectance trace, the growth rate is about 4.3 $\mu\text{m}/\text{h}$, and the thickness is about 0.8 μm . Step IV is the growth of main ZnO layer. The growth period is about 250 s, the growth rate is about 2.3 $\mu\text{m}/\text{h}$, and the ZnO thickness is about 1.5 μm . This growth rate of 2.3 $\mu\text{m}/\text{h}$ is markedly faster than that of 0.8 $\mu\text{m}/\text{h}$ using N_2O as O precursor under the growth temperature of 900 °C reported by Dadagar et al. [14], indicating a greater potential for mass production using our growth method. It should be noted that the growth rate with using H_2O as precursor is higher than that of using N_2O as precursor may be due to the following two main factors: the VI/II ratio and the growth temperature. The smaller VI/II ratio and the lower growth temperature will result in the higher growth rate. For sample B (see Fig. 2(b)), step I and step II are the same process with that of sample A. The growth time is the only difference between the step III of sample B and that of sample A. From the reflectance curves, the two samples have the same total thickness of about 2.3 μm . Compared to sample B, the swing shrinking of the trace of sample A may be resulted from the increasing of surface roughness.

Fig. 3 shows the AFM images of the two samples in a scan area of $25 \mu\text{m} \times 25 \mu\text{m}$. For sample A, very large hexagonal grains can be seen in Fig. 3(a). The mean diameter of the grains is about 8 μm , which is larger than

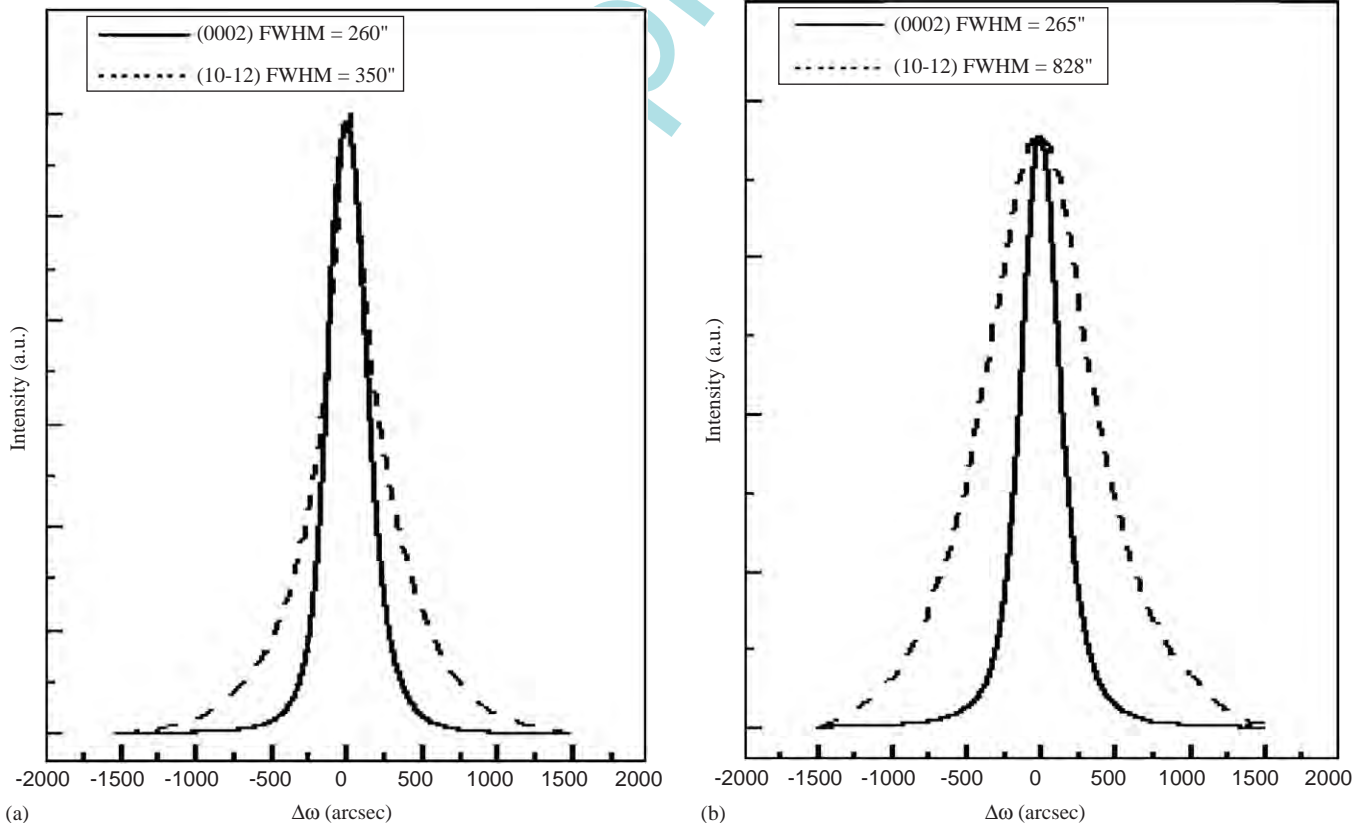


Fig. 4. The DCXRD ω -scan curves of two samples: (a) Sample A; (b) Sample B.

the grain size of about 1 μm for ZnO film with N₂O as O precursor reported by Oleynik et al. [9]. The root mean-square (RMS) roughness across this area is about 20 nm. For sample B, in agreement with the result of in-situ laser reflectance curves, a smooth surface can be seen in the Fig. 3(b) and the RMS roughness is about 2.5 nm, which is smaller than that of sample A. However, many etch pits can be seen on the surface in the AFM image of sample B, suggesting a high dislocation density in the ZnO film.

In our experiments, full-widths at half-maximum (FWHMs) of (0002) and skew (10 $\bar{1}$ 2) ω-rocking curves are used as the indicators of the screw and total dislocation densities, respectively according to the literature [15]. In Fig. 4(a), sample A has very small line-width of the rocking curves and the FWHMs of the (0002) and (10 $\bar{1}$ 2) rocking curves are 260 and 350 arcsec, respectively. The result is in agreement with the AFM result, which shows very large grain sizes. Sample B shows a significantly narrowed (0002) line width (see in Fig. 4(b)), but its (10 $\bar{1}$ 2) rocking curve is broadened. The FWHMs of the (0002) and (10 $\bar{1}$ 2) rocking curves are 255 and 828 arcsec, respectively of sample B. This result means that the screw dislocation density was kept constant but the total dislocation density was reduced significantly with using N₂O as O precursor during the growth of ZnO main layer. Compared to the ZnO film with H₂O as O-precursor, the higher growth temperature may be the main effect of N₂O gas on the quality of ZnO film. Heying et al. [15] have reported that the device-grade GaN sample with a (102) FWHM of 413 arcsec has the total threading dislocation density of 4 × 10⁸ cm⁻², so we estimate that the dislocation density of sample A is less than or in the range of 10⁸ cm⁻².

Fig. 5 shows the temperature-dependent PL spectra of two kinds of samples from 10 to 150 K. Although the trends of temperature-dependent PL spectra are the same, the difference exists in the PL spectra of them at 10 K. For sample A, it is dominated by the bound exciton peak at 3.353 eV in the Fig. 5(a) which is closer to the acceptor-bound exciton (A⁰X, i.e. I₁₀) [16]. For sample B (see Fig. 5(b)), the dominant peak is located at 3.363 eV which is usually ascribed to a hydrogen-related donor-bound exciton (D⁰X, i.e. I₄) [17], and a strong emission line at 3.331 eV originates from two-electron satellite (TES) because the luminescence line decreased together with the D⁰X (I₄) line with increasing temperature [18]. At the higher energy side, two peaks are shown at 3.372 and 3.383 eV, respectively in sample A (Fig. 5(a)). It should be noted the 3.383 eV peak shows only a shoulder. They can be attributed to the free A (FX_A) and B excitons (FX_B) due to the energy positions very close to the FX_A and FX_B observed in optical reflectance spectra of bulk ZnO crystal [19]. The little red shift of these peaks compared to bulk ZnO can be explained by exist of a tensile strain in the films. For sample B (Fig. 5(b)), two peaks at 3.374 and 3.385 eV, can be attributed to FX_A and FX_B according to the above. At the lower energy side, sample A has five peaks. The peaks at 3.161, 3.233 and 3.307 eV can be

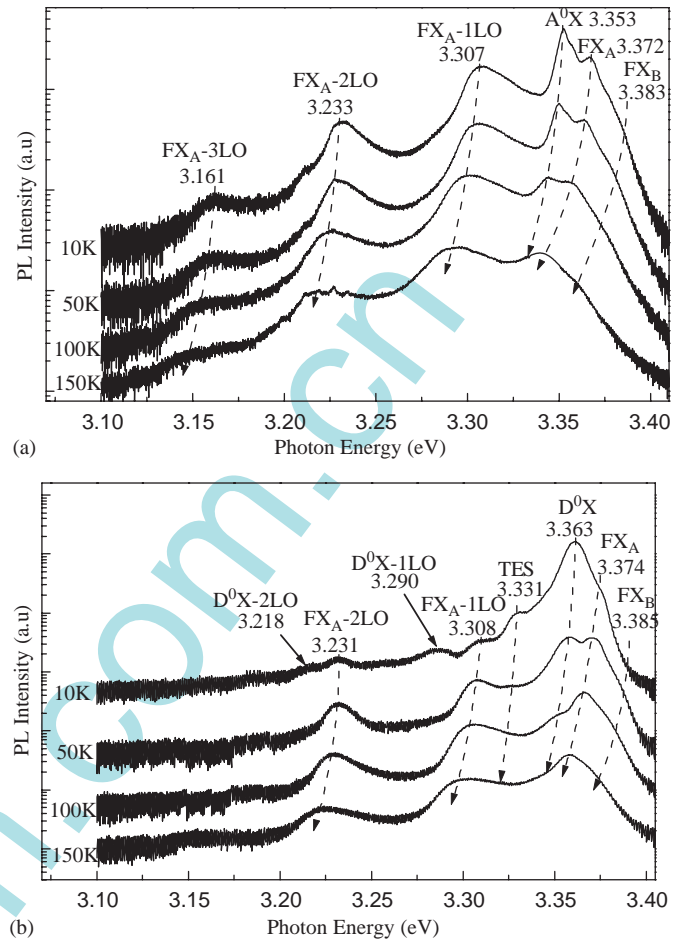


Fig. 5. Temperature-dependent PL spectra of two samples from 10 to 150 K: (a) Sample A; (b) Sample B.

attributed to 1LO, 2LO and 3LO phonon replicas of the FX_A since these lines remain up to 150 K together with the zero phonon line of FX_A the energy difference of each neighbor is close to LO phonon energy (72 meV) of ZnO calculated by Klingshirn [20] (Fig. 5(a)). To our knowledge, this is the first report of the three-phonon replicas of the FX_A of ZnO films using N₂O as O precursor. For sample B, there are four weak peaks in lower energy side. The two peaks (3.231, 3.308 eV) and another two peaks (3.218, 3.290 eV) can be attributed to 1LO and 2LO phonon replicas of the FX_A and D⁰X (I₄), respectively. From the 10 K PL spectra, the intensity ratios of FX_A to A⁰X and D⁰X for sample A and sample B are 0.55 and 0.12, respectively. Compared to sample B, the stronger FX_A and the appearance of its three-phonon replicas strongly indicate the high quality of sample A.

Table 1 shows the measured carrier concentration and electron mobility of the two samples. From the table, the carrier concentration is decreased from 2.5 × 10¹⁸ to 7.3 × 10¹⁷ cm⁻³ and the electron mobility increased from 30 to 80 cm²/Vs, respectively of sample B and sample A. The result of the improvement of electron mobility may be due to the following two main reasons: First, the dislocation density was reduced according to DCXRD

Table 1
Electrical properties of two samples

Samples	Electron concentration (cm ⁻³)	Electron mobility (cm ² /V s)
A	7.3×10^{17}	80
B	2.5×10^{18}	30

result. Second, the unintended hydrogen was eliminated according to the low PL spectra results, since a few investigations have been reported that hydrogen could act as a shallow donor in the ZnO film affect the electrical property of ZnO film [21–23].

4. Conclusion

In conclusion, we fabricated high-quality ZnO epitaxial films with AP-MOCVD using H₂O and N₂O as O precursors with the typical growth rates of 4.3 and 2.3 μm/h, respectively. The surface morphologies, crystal structures, optical and electrical properties of N₂O-grown and H₂O-grown ZnO films were investigated. By AFM measurement, the N₂O-grown ZnO film has the larger grain size and the relatively rougher surface compared to that of H₂O-grown ZnO film. The result of DCXRD show the dislocation density of the N₂O-grown ZnO film is less than that of device device-grade GaN film. From the 10 K PL spectrum of the N₂O-grown ZnO film, the A⁰X (*I*₁₀):3.353 eV dominated the spectrum and the hydrogen-related D⁰X (*I*₄):3.363 eV was disappeared. The results of DCXRD and low-temperature PL measurements show that the crystalline and optical properties of the ZnO film using N₂O as O precursor are significantly better than that of H₂O-grown ZnO film. Compared to the H₂O-grown ZnO film, the electron mobility of N₂O-grown ZnO film has been significantly improved. It should be noted that the improvement of morphology of the N₂O-grown ZnO film will be the focus of future work.

Acknowledgements

This work was supported by the National High Technology Research and Development Program of China

(863 Program) with contract No. 2003AA302160 and the Electronic Development Fund of Information Industry in China.

References

- [1] Z.K. Tang, G.K.L. Wong, P. Yu, Appl. Phys. Lett. 72 (1998) 3270.
- [2] W.Y. Liang, A.D. Yoffe, Phys. Rev. Lett. 20 (1968) 59.
- [3] A. Tsukazaki, A. Ohtomo, T. Onuma, M. Ohtani, T. Makino, M. Sumiya, K. Ohtani, S. Chichibu, S. Fuke, Y. Segawa, H. Ohno, H. Koinuma, M. Kawasaki, Nat. Mater. 4 (2005) 42.
- [4] J.Y. Park, D.J. Lee, Y.S. Yun, J.H. Moon, B.-T. Lee, S.S. Kim, J. Crystal Growth 276 (2005) 158.
- [5] A. Nahhas, H.K. Kim, Appl. Phys. Lett. 78 (2001) 1511.
- [6] Y.R. Ryu, J.M. Wrobel, H.M. Jeong, P.F. Miceli, H.W. White, J. Crystal Growth 216 (2000) 326.
- [7] C.G. van de Walle, Phys. Rev. Lett. 85 (2000) 1012.
- [8] C.G. van de Walle, Phys. Stat. Solidi (b) 229 (2002) 221.
- [9] N. Oleynik, M. Adam, A. Krtschil, J. Blasing, A. Dadgar, F. Bertram, D. Forster, A. Diez, A. Greiling, M. Seip, J. Christen, A. Krost, J. Crystal Growth 248 (2003) 14.
- [10] K. Ogata, S.W. Kim, S.Z. Fujita, S.G. Fujita, J. Crystal Growth 240 (2002) 112.
- [11] L. Wang, Y. Pu, W. Fang, J. Dai, Y. Chen, C. Mo, F. Jiang, J. Crystal Growth 283 (2005) 87.
- [12] J. Dai, H. Liu, W. Fang, L. Wang, Y. Pu, Y. Chen, F. Jiang, J. Crystal Growth 283 (2005) 93.
- [13] X.W. Sun, H.S. Kwok, J. Appl. Phys. 86 (1999) 408.
- [14] A. Dadgar, N. Oleynik, D. Forster, S. Deiter, H. Witek, J. Blasing, F. Bertram, A. Krtschil, A. Diez, J. Christen, A. Krost, J. Crystal Growth 267 (2004) 140.
- [15] B. Heying, X.H. Wu, S. Keller, Y. Li, D. Kapolnek, B.P. Keller, S.P. DenBaars, J.S. Speck, Appl. Phys. Lett. 68 (1996) 643.
- [16] B.K. Meyer, H. Alves, D.M. Hofmann, W. Kriegseis, D. Forster, F. Bertram, J. Christen, A. Hoffmann, M. Straßburg, M. Dworzak, U. Habocek, A.V. Rodina, Phys. Stat. Solidi (b) 241 (2004) 231.
- [17] K. Thonke, Th. Gruber, N. Teofilov, R. Schonfelder, A. Waag, R. Sauer, Physica B 308–310 (2001) 945.
- [18] S.W. Jung, W.I. Park, H.D. Cheong, G.-C. Yi, H.M. Jang, S. Hong, T. Joo, Appl. Phys. Lett. 80 (2002) 1924.
- [19] D.G. Thomas, J. Phys. Chem. Solids 15 (1960) 86.
- [20] C. Klingshirn, Phys. Stat. Solidi (b) 71 (1975) 547.
- [21] B. Theys, V. Sallet, F. Jomard, A. Lusson, J.-F. Rommeluere, Z. Teukam, J. Appl. Phys. 91 (2002) 3922.
- [22] A.Y. Polyakov, N.B. Smirnov, A.V. Govorkov, K. Ip, M.E. Overberg, Y.W. Heo, D.P. Norton, S.J. Pearton, B. Luo, F. Ren, J.M. Zavada, J. Appl. Phys. 94 (2003) 400.
- [23] Y.M. Strzhemechnya, H.L. Mosbacher, D.C. Look, D.C. Reynolds, C.W. Litton, N.Y. Garces, N.C. Giles, L.E. Halliburton, S. Niki, L.J. Brillson, Appl. Phys. Lett. 84 (2004) 2545.